



Hodge, R., Hoey, T., Maniatis, G., and Lepretre, E. (2016) Formation and erosion of sediment cover in an experimental bedrock-alluvial channel. *Earth Surface Processes and Landforms*, 41(10), pp. 1409-1420. (doi:[10.1002/esp.3924](https://doi.org/10.1002/esp.3924))

This is the author's final accepted version.

There may be differences between this version and the published version. You are advised to consult the publisher's version if you wish to cite from it.

<http://eprints.gla.ac.uk/116521/>

Deposited on: 24 February 2016

Enlighten – Research publications by members of the University of Glasgow
<http://eprints.gla.ac.uk>

1 **Formation and erosion of sediment cover in an experimental bedrock-alluvial**
2 **channel**

3 Rebecca Hodge¹, Trevor Hoey², Georgios Maniatis^{2,3} and Emilie Leprêtre⁴

4 ¹ Department of Geography, Durham University, Durham, UK

5 ² School of Geographical and Earth Sciences, University of Glasgow, UK

6 ³ School of Computing Science, University of Glasgow, UK

7 ⁴ Suez Environment and University of Montpellier, France

8

9 **Accepted by Earth Surface Processes and Landforms**

10

11 **Abstract**

12 Sediment grains in a bedrock-alluvial river will be deposited within or adjacent to a
13 sediment patch, or as isolated grains on the bedrock surface. Previous analysis of
14 grain geometry has demonstrated that these arrangements produce significant
15 differences in grain entrainment shear stress. However, this analysis neglected
16 potential interactions between the sediment patches, local hydraulics and grain
17 entrainment. We present a series of flume experiments that measure the influence of
18 sediment patches on grain entrainment. The flume had a planar bed with roughness
19 that was much smaller than the diameters of the mobile grains. In each experiment
20 sediment was added either as individual grains or as a single sediment pulse. Flow
21 was then increased until the sediment was entrained. Analysis of the experiments
22 demonstrates that: 1) for individual grains, coarse grains are entrained at a higher
23 discharge than fine grains; 2) once sediment patches are present, the difference in
24 entrainment discharge between coarse and fine grains is greatly reduced; 3) the
25 sheltering effect of patches also increases the entrainment discharge of isolated
26 grains; 4) entire sediment patches break-up and are eroded quickly, rather than
27 through progressive grain-by-grain erosion, and 5) as discharge increases there is
28 some tendency for patches to become more elongate and flow-aligned, and more
29 randomly distributed across the bed. One implication of this research is that the
30 critical shear stress in bedrock-alluvial channels will be a function of the extent of the
31 sediment cover. Another is that the influence of sediment patches equalises critical
32 shear stresses between different grain sizes and grain locations, meaning that these
33 factors may not need to be accounted for. Further research is needed to quantify
34 interactions between sediment patches, grain entrainment and local hydraulics on
35 rougher bedrock surfaces, and under different types of sediment supply.

37 **1. Introduction**

38 Semi-alluvial channels are identified by their predominantly bedrock channel
39 boundaries and partial alluvial cover (Turowski *et al.*, 2008). The total extent of
40 sediment cover within a semi-alluvial channel is a function of the sediment supply
41 relative to transport capacity, although the exact form of this relationship is debated
42 (Sklar and Dietrich, 2004; Turowski *et al.*, 2007; Chatanantavet and Parker, 2008;
43 Hodge and Hoey, 2012). The spatial arrangement of the sediment cover within the
44 channel is in turn the result of interactions between the bedrock topography, channel
45 hydraulics and sediment transport processes (Hodge *et al.*, 2011; Nelson and
46 Seminara, 2012; Inoue *et al.*, 2014; Johnson, 2014; Zhang *et al.*, 2015). These two
47 factors, the total extent and spatial arrangement of sediment cover, are inter-related
48 in ways that have yet to be investigated. As with alluvial bedforms, sediment patches
49 can develop in response to boundary shape (analogous to 'forced' bars in alluvial
50 literature; Seminara 2010; described as externally controlled by Wohl, 2015) or as a
51 result of the interactions between flow, bedform morphology and sediment transport
52 (equivalent to 'free' bars). To date, emphasis has been on how forced sediment
53 accumulations, whether due to irregular bedrock topography (Turowski and
54 Rickenmann, 2009; Siddiqui and Robert, 2010; Hodge and Hoey, in revision) or large
55 immobile boulders (Carling and Tinkler, 1998; Carling *et al.*, 2002; Chatanantavet
56 and Parker, 2008; Papanicolaou *et al.*, 2012) affect flow and sediment cover. To
57 interpret sediment accumulation and erosion in natural channels (e.g. Hodge and
58 Hoey, in revision) which are always likely to have a component of morphological
59 forcing of sediment cover, understanding of how self-formed 'free' bedforms function
60 in semi-alluvial channels is required.

61 The location of a grain within a semi-alluvial channel can have a significant effect on
62 that grain's critical shear stress (τ_c) and hence the ease with which it is entrained by
63 the flow. Isolated sediment grains on a smooth bedrock surface can have values of
64 τ_c that are an order of magnitude less than comparable grains in an alluvial patch
65 (Hodge *et al.*, 2011). This difference is the result of the differing pocket geometries
66 on grain exposure and pivot angle. Differences in roughness, and hence flow profiles
67 and local shear stress, over the alluvial and bedrock surfaces are also likely to
68 exacerbate differences in grain transport potential (Inoue *et al.*, 2014; Johnson,
69 2014). The spatial pattern of roughness elements in semi-alluvial channels is very
70 variable (Chatanantavet and Parker, 2008; Inoue *et al.*, 2014), complicating attempts
71 to develop empirical relationships for controls over patch development.
72 Consequently, we focus here on sediment patches on planar, relatively smooth,
73 surfaces in order to isolate the effects of grain-scale interactions on patch
74 development and erosion.

75 From the perspective of grain geometry, the distribution of isolated grains and
76 sediment patches across a bedrock surface determines the distribution of τ_c for the
77 population of grains (Hodge *et al.*, 2011), and hence the sediment flux at low
78 discharges. At higher discharges when the applied shear stress (τ) is much greater
79 than τ_c , all sediment will be fully mobile and the range of τ_c is no longer significant.
80 However, the typical lognormal distribution of flow events in a river combined with
81 low values of τ_c for isolated grains means that low flow events can have a more
82 significant impact on the total sediment flux than is the case in alluvial rivers with the
83 same sediment sizes (Lisle 1995; Hoey and Hodge, in prep). Theoretical modelling
84 has demonstrated that by distributing the same amount of sediment cover in different
85 ways (i.e. different proportions of grains in bedrock and alluvial positions) the

86 resulting average sediment fluxes range from less than to greater than the average
87 sediment flux in a comparable alluvial river (Hoey and Hodge, in prep). An
88 understanding of the development of sediment cover in semi-alluvial channels is
89 therefore necessary in order to predict sediment fluxes in these systems.

90 There is little empirical data with which to constrain the most likely distributions of
91 sediment cover, however, previous research has identified some first order
92 tendencies. Higher values of τ_c for grains in alluvial patches are likely to produce a
93 net flux of grains from bedrock surfaces to alluvial patches (Nelson and Seminara,
94 2012). Sediment is thus most likely to form alluvial patches, with only a small fraction
95 of the grains remaining isolated on bedrock surfaces. This pattern is consistent with
96 field sediment tracer data (Hodge *et al.*, 2011). The position and form of alluvial
97 patches will be controlled by both the underlying bedrock topography and
98 interactions between the patch roughness and the local hydraulics (Finnegan *et al.*,
99 2007; Johnson and Whipple, 2010; Hodge and Hoey, in revision). Alluvial bedforms
100 such as pebble clusters affect the local hydraulics, causing a downstream separation
101 zone and coherent flow structures with well-defined spatial characteristics (Strom
102 and Papanicolaou, 2007; Lacey and Roy, 2008). Similar processes will occur around
103 alluvial patches, amplified by the potential contrast in roughness between bedrock
104 and alluvial regions and the topographic expression of patches on a bedrock surface,
105 so affecting the growth and shape of the patches and local sediment transport.
106 Whether flow conditions are steady or varying, it is unclear how the bedforms
107 interact and whether these interactions are predominantly regenerative (maintaining
108 bedforms of a given size) or constructive (tending to merge bedforms into a smaller
109 number of larger features) (Kocurek *et al.*, 2010).

110 To begin to address the issues raised above, in this paper we present results from
111 flume experiments on the development and erosion of sediment cover on a bedrock
112 surface. We simplify conditions to assess the fundamental process controls over free
113 bedforms, and use uniform channel width, slope and roughness. In each experiment,
114 a fixed volume of sediment was introduced at the upstream end of a flume with a
115 plane bed of constant low roughness, which resulted in sediment patches
116 developing. Once sediment cover had developed, flow was increased at a known
117 rate and the sediment cover was eroded. The aims of the experiments are to: 1)
118 quantify the impact of grain size and position on τ_c , which is recorded by the flow at
119 which different grains are entrained; and, 2) quantify patch geometry and how this
120 changes as patches are eroded. Results are reported from three sets of
121 experiments: Set 1, control experiments using single grains and no sediment
122 patches; Set 2 with a uniform coarse grain size; and Set 3 with different mixtures of
123 two uniform sediments, one coarse and one fine.

124 **2. Methods**

125 Three sets of experiments (Sets 1, 2 and 3; Table 1) were carried out in a 0.9 m wide
126 flume which has a working length of 8 m and maximum flow of 75 l s^{-1} . A flat plywood
127 bed was installed in the flume, with small-scale roughness added by fixing a layer of
128 $< 0.5 \text{ mm}$ sand to this using varnish. Flume slope was 0.0067 (Sets 1 and 3) and
129 0.0050 (Set 2). Uniform flow was established throughout the operational section at
130 the start of each run by setting discharge to be close to the sediment transport
131 threshold and adjusting the elevation of the flume tail gate until water depth was
132 constant through the measuring section. Under the initial low flow conditions, flow
133 depths varied from 9 to 40 mm. As flow increased, maximum flow depths were
134 between 50 and 80 mm. Flow properties vary according to the sediment cover on the

135 bed. With no sediment cover, flows across the experimental range of 8.5 to 40 l s⁻¹
136 had a Froude number between 1.27 and 1.33, and Reynolds number of 9100 to
137 40300. As sediment patches develop, flow may become subcritical. Under the
138 extreme condition of full sediment cover (which is more cover than seen in the
139 experiments), flows from 5.4 to 33 l s⁻¹ have Froude numbers between 0.20 to 0.48
140 and Reynolds numbers from 5400 to 30300.

141 Figure 1 outlines the experimental procedure. Set 1 experiments (Table 1) were a
142 control to measure the entrainment threshold for the material used in later
143 experiments when introduced as single, isolated grains. Two very angular sediments
144 (0.2 on the Krumbein roundness scale; Krumbein, 1941) with uniform grain sizes
145 were used for the experiments. Coarse sediment (C) has $D_{50}=15$ mm and fine
146 sediment (F) has $D_{50} = 8.5$ mm. In each Set 1 experiment a single, randomly
147 selected, grain was placed on the centreline of the flume ~4 m from the flume
148 entrance and flow was increased until the grain was entrained. Fifty measurements
149 were made, twenty five with each of the fine and coarse grains.

150 In Set 2 and 3 experiments, a known volume of sediment was introduced at the initial
151 discharge, and allowed to developed patches of sediment cover in the measurement
152 section which extended from 5.5 to 5.8 m along the flume and across the entire width
153 of the flume (a total area of 0.27 m², determined by the video camera field of view).
154 Sediment cover in the measurement area was representative of that in the rest of the
155 flume. Furthermore, each experiment was repeated at least three times. The initial
156 discharge was maintained until there was little temporal variation in cover extent,
157 which typically took about 15 min to form. Sediment cover extent ranged from 13% to
158 23%. Flow was then increased at a rate of 1.2 l s⁻¹ per minute until the maximum
159 capacity of the pump was reached to erode the sediment grains and patches. Patch

160 formation and erosion was recorded by vertical video photography. Set 2 consisted
161 of 21 repeat experiments each using 20 kg of coarse sediment C. Set 3 used the
162 sediments C and F mixed in the following proportions (where the numbers refer to
163 the percentage of each size fraction in the mixture): 100C, 75C/25F, 50C/50F,
164 25C/75F, 10C/90F and 100F. Each set 3 experiment used 6 kg of sediment,
165 although the proportion of this that formed sediment patches the measuring section
166 varied between runs. Up to 5 repeats were performed of each experiment in Set 3.

167 Two main approaches were used to analyse the video of the experiments in Sets 2
168 and 3. The first was watching the erosion of the sediment cover, and identifying the
169 time and hence discharge at which isolated grains, and those in patches, were
170 eroded. Isolated grains were defined as being those with contact with ≤ 2 other
171 grains in Set 2, and as one grain diameter from any other grain in Set 3. These
172 different definitions reflect differences in the typical behaviour of the coarse and fine
173 grains. In runs with both coarse and fine grains, patches were classified by grain
174 sizes within the patch (coarse, fine or mixed). The analysis noted the time (and
175 hence discharge), of the first entrainment of isolated grains (defined as three grains
176 moving a distance of one or more grain diameters), and the first break up of a stable
177 alluvial patch. In Set 3, the timing of the entrainment of all grains within the imaged
178 area was also recorded. In both sets grains entering the frame from upstream were
179 ignored.

180 The second analytical approach was to measure the sediment cover and the patch
181 geometry. Stills from the videos of the experiments were analysed using two different
182 methods. In the first, the software ImageJ (<http://imagej.nih.gov/ij/index.html>) was
183 used to segment automatically the grains from the background using the Trackmate
184 algorithm (Crocker and Grier, 1996). Isolated grains were manually identified, and

185 their areas calculated by the software. The algorithm results were visually assessed
186 to ensure that grains were being identified correctly. The segmentation algorithm
187 was applied to images of high flows over an empty bed to quantify phantom cover
188 caused by scattered light, and this amount of cover was removed from the total
189 calculated from subsequent images. In the second approach, grains were digitised
190 by manually marking the centre of every grain in the frame, and identifying whether
191 the grain was fine or coarse. Image aberration due to the water surface was not
192 explicitly accounted for because it was possible to visually identify the location of all
193 grains.. All grains within one grain diameter were identified as being members of the
194 same patch, and isolated grains were those that were more than one grain diameter
195 from any neighbouring grain (Figure 1).

196 The two techniques give comparable estimates of the proportion of sediment cover,
197 with the RMS error between estimates from 65 frames being 0.026. The similarity
198 between the two sets indicates that the automated segmentation techniques are
199 robust. In Set 2 experiments, changes in the proportion of sediment cover were
200 assessed in 142 frames using Image J. In Set 3 experiments, digitisation of grains
201 was carried out on twelve runs; two of each sediment mixture. For each run, frames
202 from one, five and every subsequent five minute interval after the onset of the flow
203 increase were analysed.

204 A number of patch statistics were calculated from the digitised Set 3 images:
205 dimensions, orientation and Ripley's K statistic. Patch dimensions were calculated
206 using the Matlab function `regionprops`, which fits an ellipse with the same second
207 moments as the patch area (where the second moment of an area reflects the
208 distribution of material within the area), and provides the major and minor axis
209 lengths and major axis orientation. This method takes into account all sediment

210 within the patch, rather than just at the extremes as a bounding box approach would
 211 do, and provides an estimate of patch size that is less sensitive to patch shape.
 212 Ripley's K statistic is a measure of how points are distributed across a surface,
 213 describing whether points are more evenly distributed or more clustered than a
 214 random spacing (Hajek *et al.*, 2010; L'Amoreaux and Gibson, 2013). The K statistic
 215 is calculated at a range of lags in order to identify whether the distribution changes
 216 as a function of spatial scale. The statistic is estimated for lag r (defined here as a
 217 number of grain diameters) using:

$$218 \quad \hat{K}(r) = \frac{1}{\hat{\lambda}N} \sum_{\substack{i=1 \\ i \neq j}}^N \sum_{j=1}^N w(s_i, s_j)^{-1} \partial_{ij}(r) \quad [1]$$

219 (Cressie, 1991; L'Amoreaux and Gibson, 2013) where N is the total number of
 220 events in the study area, $\hat{\lambda}$ is the density of events in the study area, and s_i, s_j are
 221 two different events within the area. The weighting factor $w(s_i, s_j)$ accounts for edge
 222 effects and ∂_{ij} serves as a counting function being 1 when the distance between s_i
 223 and s_j is ≤ 1 , otherwise $\partial_{ij} = 0$. K is then re-scaled using:

$$224 \quad \hat{L}(r) = (\hat{K}(r)/\pi)^{0.5} - r \quad [2].$$

225 A spatially random distribution has $\hat{L}(r) = 0$ and values > 1 indicate more clustering
 226 and values < 1 more regular spacing, than a random distribution. A Monte Carlo
 227 approach is used to calculate a confidence interval for the K statistic. For each
 228 digitised image, 100 datasets with the same number of points as the image, but with
 229 the points at random locations are produced. K statistics at different spatial lags are
 230 calculated for these datasets, and the 2.5th to 97.5th percentile envelope of these
 231 lags produces a 95% confidence interval.

232 **3. Results**

233 3.1. Grain entrainment shear stress

234 Results of the conditions under which grain entrainment occurred are mainly
235 reported in terms of discharge, rather than shear stress. The shallow flow depths
236 relative to the grain size produced non-uniform flow over the sediment patches,
237 meaning that du Boys' approximation of shear stress is not applicable for Sets 2 and
238 3. However, in Set 1 the single isolated grains did not significantly disrupt the uniform
239 flow in the flume, and so du Boys' approximation is valid. Flows were also too
240 shallow to measure local velocity profiles that could be used to calculate shear
241 stress.

242 Figure 2 shows the distributions of discharge at which isolated grains and alluvial
243 patches first began to move in experimental Sets 1 and 2. In Set 1, fine and coarse
244 isolated grains move at mean discharges of $5.8 (\pm 0.31) \text{ l s}^{-1}$ (one standard error) and
245 $8.3 (\pm 0.81) \text{ l s}^{-1}$ respectively. These are equivalent to shear stresses of $0.95 (\pm 0.02)$
246 and $1.12 (\pm 0.05) \text{ Pa}$, and dimensionless shear stresses of $0.007 (\pm 0.0002)$ and
247 $0.004 (\pm 0.0002)$. These entrainment discharges for the coarse and fine grains are
248 significantly different (t-test, $p = 0.007$).

249 In Set 2, isolated coarse grains start to move at a discharge of 10 l s^{-1} , with coarse
250 grains in patches beginning to move at a significantly higher discharge of 21 l s^{-1} (t-
251 test, $p < 0.0001$). Entrainment discharges of isolated coarse grains in Set 2 are higher
252 than for isolated coarse grains in Set 1, although this is not statistically significant (t-
253 test, $p = 0.057$). This 20% increase in discharge between Sets 1 and 2 is equivalent
254 to approximately a 10% rise in shear stress (assuming that shear stress is
255 proportional to flow depth and that this scales with $Q^{0.5}$, and remembering that du
256 Boys' approximation cannot be applied to Set 2).

257 Distributions of entrainment shear stresses from Set 3 are shown in Figure 3. In
258 these boxplots, data from the different replicate runs are amalgamated. Such
259 amalgamation is supported by application of the Kruskal-Wallis test, which was used
260 to compare the entrainment discharge for grains of the same size and in the same
261 location between different replicates. In 6 out of the 23 combinations of sediment
262 mixture and grain position, there was no significant difference ($p > 0.05$) between
263 any of the different replicate runs. In 14 of the other combinations, application of
264 Tukey-Kramer revealed that within each set of replicates, only one distribution was
265 significantly different to the other ones.

266 In Set 3, across all sediment mixtures, fine grains in both isolated and patch
267 locations start to be entrained at a discharge of around 9 l s^{-1} (Figure 3). Coarse
268 grains in isolated and patch locations show a similar behaviour when there is up to
269 50% fines in the sediment mixture, and this behaviour is comparable to the
270 behaviour of the coarse grains in Set 2. However, when more than 50% of the
271 mixture is fine sediment, coarse isolated grains and coarse patches start to be
272 entrained at higher discharges. Figure 3 also shows the variation in initial
273 entrainment between replicate runs. Across all sediment mixtures, isolated fine
274 grains have initial entrainment over a range of 3.6 l s^{-1} , whereas for coarse isolated
275 grains there is more variability and the range is 7.6 l s^{-1} . There is most variability in
276 the initial entrainment from fine and coarse patches, with ranges of 19.7 and 19.6 l s^{-1} .
277 Initial entrainment from mixed patches has similar values and range to that of
278 coarse isolated grains. Such variability in initial motion is consistent with that
279 observed in the field by Richardson *et al.* (2003).

280 Consolidating the above interpretation (Figure 3), the Kruskal-Wallis test indicates a
281 significant difference ($p < 0.05$) between the minimum discharges for different grain

282 sizes and positions in runs 100C/0F, 10C/90F, 50C/50F and 25C/75F. Additional use
283 of the Tukey-Kramer test confirms that the main differences are between patch and
284 isolated grains. An alternative grouping of the data by grain size and location, and
285 hence comparison between sediment mixtures, showed that the only significant
286 variation in minimum discharge with sediment mixture is for coarse isolated grains.

287 In Set 3, grain size and location affects the discharge (value and variability) at initial
288 grain entrainment. In contrast, the mean discharge at which grains are entrained is
289 less variable between different grain sizes and locations. As before, there is most
290 variation in the replicate runs for grains in fine and coarse patches. Grains in these
291 patches are also the most affected by the composition of the sediment mixture; as
292 the percentage of fines increases, the mean entrainment shear stress for grains in
293 fine and coarse patches decreases and increases respectively.

294 Application of the Kruskal-Wallis test to the full distributions of entrainment
295 discharges for all mobile grains revealed that for each sediment mixture, there were
296 significant differences between grains in different locations ($p \leq 0.02$). Further
297 analysis with Tukey-Kramer revealed that in all cases the significant differences were
298 between grains in isolated and patch positions. For each sediment mixture, there
299 was no significant difference between the distributions of entrainment discharge for
300 coarse and fine isolated grains if both were present. For each mixture there was also
301 no significant difference between grains in the various types of patches, with the
302 exception of the fine and mixed patches in 10C/90F.

303 The analysis of sediment entrainment has demonstrated that: 1) the impact of grain
304 size on entrainment discharge become less important once there are sediment
305 patches present; 2) the presence of sediment patches increases the entrainment

306 discharge for isolated grains as well as for patch grains, indicating the impact of
307 patches on hydraulics; 3) grain location has a greater impact on the minimum
308 entrainment discharge than on the mean; and 4) fine and coarse patches become
309 relatively less and more stable respectively as the proportion of fines in the sediment
310 mixture increases.

311 **3.2. Erosion of sediment cover**

312 The extent of sediment cover at steady state was an average of 22.4 (± 0.24)% (one
313 standard error) in Set 2 experiments and 15.6 (± 0.6)% in Set 3 experiments. In Set 3
314 runs, over 80% of initial sediment cover was in patches. This proportion decreased
315 as the sediment was eroded. In Set 3, the extent of sediment cover did not vary
316 systematically with the proportions of coarse and fine sediment, although the most
317 extensive covers were produced by mixtures of coarse and fine sediment. As
318 discharge increased, erosion decreased the areal extent of sediment cover. In Set 2
319 experiments, the total area occupied by patches remained approximately constant
320 until a discharge of $\sim 20 \text{ l s}^{-1}$, after which the area decreased approximately linearly.
321 Erosion of isolated grains commenced as soon as discharge began to increase, and
322 no isolated grains remained once discharge exceeded 25 l s^{-1} . Set 3 experiments
323 show a similar overall pattern, although the areal extent of patches begins to
324 decrease as soon as the discharge begins to rise rather than only after a threshold
325 value as in Set 2. As in Set 2, isolated grains in Set 3 are mostly removed by a
326 discharge of 25 l s^{-1} . In both Set 2 and Set 3, there is variability between runs,
327 reflecting specific grain arrangements that occurred as the patches developed.

328 **3.3. Sediment patch geometry**

329 The digitised grain data from the Set 3 experiments show how patch geometry
330 (number, area, orientation and elongation) changed during erosion (Figure 5). As the

331 patches are eroded, there is a systematic decline in the number of patches (Figure
332 5a), and the remaining patches become more flow-aligned (Figure 5c). In most runs
333 there is a concurrent decrease in patch area (Figure 5b), but this decrease is less
334 consistent between the different runs. Finer sediment mixtures tend to have more,
335 smaller, patches. Average patch elongation (major:minor axis length, Figure 5d) has
336 an initial value of 2.4 in all runs. As erosion occurs, elongation generally remains
337 between 2 and 3, apart from a small number of runs in which significantly more
338 elongate patches develop when discharge $> 20 \text{ l s}^{-1}$.

339 Within-run analysis of these properties (Figure 6) shows considerable variability on
340 top of the trends in Figure 5. In some cases there is an observable change in the
341 distribution of patch properties as discharge increases and patches are eroded
342 (Figure 6a and b); and in other cases the distributions remain the same (Figure 6c).
343 In most runs the size of the largest patch decreases with increasing discharge.
344 Changes in the distribution of patch orientation with increasing discharge are
345 statistically significant in four of the twelve digitised runs ($p < 0.05$; Kruskal-Wallis
346 test). Changes in the distributions of patch elongation and area were only each
347 statistically significant in one of the twelve runs ($p < 0.05$; Kruskal-Wallis test). There
348 is no systematic relationship between how patch properties change as patches are
349 eroded, and the composition of the sediment mixture.

350 The decrease in number of patches and consistent patch area suggest that as the
351 primary erosion mechanism is the removal of entire patches, rather than patches
352 becoming smaller through erosion round the edges. The change in patch orientation
353 indicates some preferential erosion and local reworking, with grains being removed
354 from patch flanks and deposited in downstream lee locations. The heterogeneity of
355 patch behaviour demonstrates the influence of patch position relative to other

356 patches, with sediment from upstream erosion potentially resulting in simultaneous
357 accretion and erosion.

358 The interactions between sediment patches and local hydraulics will affect the spatial
359 distribution of grains across the bed. This distribution is quantified using Ripley's L
360 statistic. At one minute into the increase in discharge, variations in $L(r)$ as a function
361 of spatial lag (Figure 7) show that at lags equivalent to one or two coarse grain
362 diameters, values of $L(r)$ are significantly negative. Such values indicate that grains
363 are more dispersed than a random distribution. This is partly because the diameter
364 of the grains determines the minimum distance between grain centres, whereas in
365 the random simulations there is no minimum distance between points. The result
366 may also indicate that there is a minimum spacing between grains in the flume, i.e.
367 that grains are not in contact. For all sediment mixtures, at lags greater than about
368 three grain diameters, there is a rapid transition to significant positive $L(r)$ values,
369 indicating clustering of the grains in patches.

370 The distribution of $L(r)$ changes as the sediment patches are eroded (Figure 8 and
371 Figure 9); examples are shown from 100C/0F and 50C/50F, but the overall trends
372 are common to all runs. As the patches are eroded, $L(r)$ starts to decrease. In run
373 100C/0F (Figure 8), sediment grains are randomly distributed by 20 minutes into the
374 increasing flow regime. Run 50C/50F, shows the same trend for reduced clustering,
375 although the values of $L(r)$ are still above the simulated confidence interval at 25
376 minutes. The reduction in $L(r)$ starts at the larger lags, indicating that grains are
377 becoming less clustered at this spatial scale, but retaining their clustering at smaller
378 scales. This suggests that the erosion of entire sediment patches dominates over
379 grain-by-grain erosion processes. If the latter process were dominant, $L(r)$ would
380 decrease at smaller, as well as larger, lags. The interpretation of Figure 7, Figure 8

381 and Figure 9 is thus that there is clustering between the initial patches, but as
382 erosion proceeds and patches are removed the spacing of the patches becomes
383 more random. There are not, however, changes to the clustering of sediment grains
384 within a patch.

385 **4. Discussion**

386 **4.1. Controls on grain entrainment**

387 Data from the three sets of experiments show that when sediment patches are
388 present, the location of a grain in either an isolated or a patch position has a larger
389 impact on the discharge at which it is entrained than does its diameter (Figure 3).
390 The difference between isolated fine and coarse grains is far greater in the control
391 experiments with single grains (Set 1) than in Set 3 when patches are present.
392 Furthermore, the presence of patches also affects the discharge at which isolated
393 grains are entrained, with isolated coarse grains being entrained at higher
394 discharges in Set 2 than in Set 1 (Figure 2). This small but notable effect is evidence
395 of the impact of sediment patches on hydraulic conditions across the measurement
396 area. The impact of sediment patches is therefore twofold; grains in the patches
397 have an increased critical shear stress through the combined effects of changed flow
398 hydraulics and inter-grain friction, but isolated grains also have a reduced mobility as
399 a result of the significant secondary effect of patches in changing the reach-scale
400 hydraulics.

401 The impact of patch formation may be greater for the fine isolated grains, as
402 expressed by the proportionally larger increase in discharge between Sets 1 and 3
403 because their size makes them more likely to be sheltered from the flow by upstream
404 patches. The spatially variable pattern of shear stresses experienced by the isolated
405 grains which results from the arrangement of other grains on the bed is displayed in

406 the difference between the minimum and mean discharges at which isolated grains
407 are entrained (Figure 3). In Set 3, isolated fine grains have the largest difference
408 between minimum and mean discharge, indicating that although many grains are
409 affected by the patches, some grains still occupy areas of the bed with similar
410 hydraulics to those in Set 1. For the coarse isolated grains and all patches, there is a
411 smaller, but notable, difference between the minimum and mean discharges,
412 indicating that there is a similar level of local shear stress variation within the patches
413 as there is in the areas surrounding them. Furthermore, the mean discharges are
414 similar in all locations, meaning that once the impact of grain geometry is accounted
415 for, the forces experienced by grains in a patch could actually be higher than those
416 experienced by isolated grains at the same discharge. This impact of the patch
417 geometry on the flow, and the overriding of grain size effects, is similar to that
418 observed in steep channels with immobile boulders by Yager *et al.* (2012), who also
419 found that sediment patch grain size was not always a good predictor of sediment
420 mobility. The experiments also show that the sediment composition had an impact
421 on the stability of fine and coarse patches, with patches being most stable when their
422 composition is most different to the bulk composition (e.g. fine patches are most
423 stable at 75C/25F). For fine grains, it follows that as the sediment coarsens, the
424 relative roughness of the bed will increase, and patches of fine sediment will become
425 relatively more sheltered. For coarse patches the phenomenon is harder to explain,
426 as coarse grains will become relatively more exposed as the sediment mixtures fine,
427 but may be related to the tendency of the finer sediment to form more numerous,
428 smaller, patches (Figure 5), which may more consistently increase roughness across
429 the entire measurement area.

430 **4.2. Sediment cover and patch geometry**

431 As the sediment cover is eroded, sediment patches are removed through the erosion
432 of discrete patches, and the distribution of patches across the bed becomes more
433 random. There is also some evidence that patches become more elongate and
434 aligned with the flow direction. The interaction between patches is constructive
435 (Kocurek *et al.*, 2010), and elements of merging, cannibalization and remote transfer
436 are all seen in our experiments. However, our experiments are limited to short
437 reaches and there is no upstream feed of sediment during erosion. Should a
438 continuous feed, at a rate equal to the erosion rate from the observed reach, be
439 introduced then regeneration and self-organisation of the bedforms may occur.

440 The form of the equilibrium between patch size, flow and sediment supply is likely to
441 involve different bedform geometries under different boundary conditions (Nelson *et al.*,
442 2009; Dreano *et al.*, 2010; Hodge, in press), so cannot be predicted from present
443 experiments. The process of patch removal suggests that patches may be sensitive
444 to the entrainment of key grains, either in the patch or an upstream location, which
445 change the local hydraulics and/or grain geometry. Positive feedback by which the
446 erosion of grains destabilises surrounding grains means that a patch can be rapidly
447 removed, as has been reported for particle clusters in alluvial rivers (Strom *et al.*,
448 2004; Tan and Curran, 2012; Heays *et al.*, 2014). Further analysis of the videos
449 could attempt to identify the size and locations of these grains.

450 **4.3. Feedbacks between flow and sediment patches**

451 The development and erosion of sediment patches is a function of the feedbacks
452 between flow, bed morphology and sediment transport (Werner, 2003; Kocurek *et al.*
453 *et al.*, 2010). These experiments have demonstrated that under the idealised conditions
454 in the flume, sediment patches can override the effects of grain size on grain
455 entrainment, and can influence entrainment conditions in locations beyond the patch,

456 as well as within the patch itself. Consequently, the patches act to equalise the
457 development and erosion of sediment cover across a range of sediment mixtures.
458 The range of entrainment discharges demonstrated by both isolated and patch
459 grains indicates that the patches induce spatial variation in flow conditions, both
460 within and between the patches. As such these results provide some insight into the
461 mechanisms by which patches self-organise, and provide physical support for rule-
462 based models that have demonstrated the formation of such patches and other
463 coarse bedforms (Werner and Fink, 1993; Hodge and Hoey 2010).

464 The observed impact of sediment patches on the critical grain entrainment discharge
465 might suggest that with continual sediment supply, extensive sediment cover can
466 rapidly develop as a result of runaway feedback mechanisms (Chatanantavet and
467 Parker, 2008; Hodge and Hoey, 2010). Such cover does not occur in these
468 experiments because of the limited duration and volume of sediment input. The
469 erosion of sediment cover demonstrates the same mechanism in reverse, with rapid
470 destabilisation of sediment patches. These mechanisms suggest that bedrock-
471 alluvial rivers would tend to have binary sediment cover, with either limited or
472 extensive cover, in the absence of larger-scale roughness elements that drive forced
473 patch (bar) formation.

474 However, in these experiments, the bed developed a stable sediment cover of
475 around 25% under the initial input conditions; the consistency between experiments
476 in set 2 provides evidence that this was an equilibrium configuration. The
477 development of this cover demonstrates that a relatively low spatial density of
478 sediment grains is necessary to disrupt the hydraulics and create conditions suitable
479 for the maintenance of that cover. This could suggest that under the limited and/or
480 intermittent sediment supply common to many bedrock-alluvial rivers (Lague, 2010),

481 partial sediment covers may be common. This is further supported by the spatially
482 variable conditions induced by the sediment cover. The observed grain entrainment
483 will reflect the conditions of areas of the bed where grains were initially deposited,
484 i.e. those with lower flow velocities. The areas between the grains may be subject to
485 local flow acceleration as a result of grain blockages in other locations, which would
486 discourage deposition in these areas and the development of complete sediment
487 cover. Such preferential pathways for bedload transport have also been observed in
488 the field and flume under conditions of reduced sediment supply (Richardson *et al.*,
489 2003; Nelson *et al.*, 2009).

490 **4.4. Implications for bedrock-alluvial rivers**

491 These experiments demonstrate that even a relatively low density of sediment grains
492 can have a significant impact on flow hydraulics and sediment patch development.
493 Consequently, relatively small inputs of sediment into a channel could have notable
494 impacts on channel roughness, flow and sediment transport. The importance of the
495 development of patches will depend on the channel topography, with patches being
496 likely to have less of an impact in channels with a rougher bedrock topography
497 (Inoue *et al.*, 2014; Johnson, 2014). Under rough topographies, sediment patch
498 development could instead smooth the channel bed, producing a different set of
499 feedbacks. However, even within a channel with a grain-rough (*sensu* Inoue *et al.*,
500 2014) topography, there will still be areas of the bed that are locally flat at a scale
501 larger than that of the sediment grains, and in these locations the relationships these
502 experiments are likely to still apply.

503 These experiments have demonstrated that a single pulse of sediment can produce
504 a partial sediment cover. There are questions as to how this behaviour upscales to a
505 bedrock river with a fluctuating discharge and sediment supply. There are also

506 questions about the interactions between flow, sediment cover and sediment
507 entrainment under conditions of greater partial cover. The extent to which sediment
508 patches disrupt the flow is likely to be a non-linear process, with maximum disruption
509 occurring once a large proportion of the bed is affected by the wakes from patches.
510 As cover increases further, the bed will effectively become smoother again, reducing
511 the disruption.

512 These experiments also have implications for predicting sediment transport in
513 bedrock-alluvial rivers. The limited impact of grain size on grain entrainment in the
514 experiments with patches is consistent with previous observations that in channels
515 with partial sediment cover, sediment transport is independent of grain size (Hodge
516 *et al.*, 2011). In addition to potentially disregarding grain size, the experiments also
517 suggest that, in a mixture of isolated and patch grains, it may be appropriate to use a
518 single entrainment shear stress for both; however, this is not the case if the two
519 populations occur in distinct areas of the bed. The experiments do, however, suggest
520 that the magnitude of the critical shear stress will be a function of the extent of
521 sediment cover.

522 **5. Conclusions**

523 These experiments show that under idealised conditions (flat bed and maximum of
524 two grain sizes) the production and erosion of sediment patches on a flat surface is
525 affected by complex interacting processes. Isolated sediment grains away from the
526 influence of any other sediment are entrained at lower discharges than grains in
527 sediment patches. However, when sediment patches have formed in the flume,
528 isolated grains are entrained at a comparable mean discharge to grains in the
529 sediment patches. This is because of the influence of the sediment patches on the
530 local flow conditions.

531 The rate at which sediment patches are eroded as discharge is increased is
532 approximately linear. The main reduction in sediment cover is through removal of
533 entire patches, rather than grain-by-grain removal from patches. Sediment patches
534 are reshaped as erosion progresses, becoming more flow orientated and sometimes
535 more elongate. Grains are clustered at lags equivalent to a small number of grain
536 diameters, but over time grain spacing at larger lags becomes more random.

537 Increasing understanding of the way in which sediment cover is produced and
538 eroded on flat bedrock surfaces requires further research on the impact of sediment
539 grains on the local flow, and consequent feedbacks on sediment transport
540 processes. When there is an amount of sediment on the bed, these feedbacks
541 appear to be the dominant control on patch stability, overriding the impact of grain
542 size and whether grains are isolated or in a cluster.

543 **Acknowledgements**

544 Experiments in the hydraulics laboratory, University of Glasgow, had technical
545 support from Stuart McLean, Tim Montgomery and Kenny Roberts, and additional
546 help from Callum Pearson and Rebecca Smith. We thank that AE and two reviewers
547 for their useful comments.

548

549 **References**

550 L'Amoreaux, P., and S. Gibson (2013), Quantifying the scale of gravel-bed clusters
551 with spatial statistics, *Geomorphology*, 197, 56–63,
552 doi:10.1016/j.geomorph.2013.05.002.

553 Carling P. A., Hoffmann M. and A. S. Blatter (2002). Initial motion of boulders in
554 bedrock channels. In: *Ancient Floods, Modern Hazards: Principles and Applications*

555 of Paleoflood Hydrology, *Water Science and Application* Volume 5, pages 147-160,
556 AGU.

557 Carling P. A. and K. Tinkler (1998). Conditions for the entrainment of cuboid
558 boulders in bedrock streams: An historical review of literature with respect to recent
559 investigations. In: *Rivers over Rock*, AGU. Chatanantavet, P., and G. Parker (2008),
560 Experimental study of bedrock channel alluviation under varied sediment supply and
561 hydraulic conditions, *Water Resour. Res.*, 44(12), doi:10.1029/2007WR006581.

562 Cressie, N.A.C. (1991) *Statistics for Spatial Data*, Wiley, New York.

563 Crocker, J.C., and D.G. Grier (1996), Methods of digital video microscopy for
564 colloidal studies, *Journal of Colloid and Interface Science*, 179(1) 298-310.

565 Dreano J., Valance A., Lague D. and C. Cassar (2010). Experimental study on
566 transient and steady-state dynamics of bedforms in supply limited configuration.
567 *Earth Surf. Process. Landforms* 35, 1730-1743, doi: 10.1002/esp.2085

568 Finnegan, N. J., L. S. Sklar, and T. K. Fuller (2007), Interplay of sediment supply,
569 river incision, and channel morphology revealed by the transient evolution of an
570 experimental bedrock channel, *J. Geophys. Res.*, 112(F3),
571 doi:10.1029/2006JF000569.

572 Hajek, E. A., P. L. Heller, and B. A. Sheets (2010), Significance of channel-belt
573 clustering in alluvial basins, *Geology*, 38(6), 535–538, doi:10.1130/G30783.1.

574 Heays, K. G., H. Friedrich, and B. W. Melville (2014), Laboratory study of gravel-bed
575 cluster formation and disintegration, *Water Resources Research*, 50(3),
576 doi:10.1002/2013WR014208.

577 Hodge, R. A. (in press), Sediment processes in bedrock-alluvial rivers: Research
578 since 2010 and modelling the impact of fluctuating sediment supply on sediment
579 cover, *Gravel Bed Rivers 8: Gravel Bed Rivers and Disasters*, edited by J. Laronne
580 and D. Tsutsumi, Wiley.

581 Hodge, R. A., and T. B. Hoey (2012), Upscaling from grain-scale processes to
582 alluviation in bedrock channels using a cellular automaton model, *Journal of*
583 *Geophysical Research: Earth Surface*, 117, F01017, doi:10.1029/2011JF002145.

584 Hodge R. A., and T. B. Hoey (in revision), The impact of topography in a bedrock-
585 alluvial channel: 2. Sediment cover, *J. Geophys. Res.*,

586 Hodge, R. A., T. B. Hoey, and L. S. Sklar (2011), Bedload transport in bedrock
587 rivers: the role of sediment cover in grain entrainment, translation and deposition, *J.*
588 *Geophys. Res.*, doi:10.1029/2011JF002032.

589 Inoue, T., N. Izumi, Y. Shimizu, and G. Parker (2014), Interaction among alluvial
590 cover, bed roughness and incision rate in purely bedrock and alluvial-bedrock
591 channel, *J. Geophys. Res. Earth Surf.*, 2014JF003133, doi:10.1002/2014JF003133.

592 Johnson, J. P. L. (2014), A surface roughness model for predicting alluvial cover and
593 bed load transport rate in bedrock channels, *J. Geophys. Res. Earth Surf.*,
594 2013JF003000, doi:10.1002/2013JF003000.

595 Johnson, J. P. L., and K. X. Whipple (2010), Evaluating the controls of shear stress,
596 sediment supply, alluvial cover, and channel morphology on experimental bedrock
597 incision rate, *J. Geophys. Res.*, 115, F02018, doi:201010.1029/2009JF001335.

598 Kocurek, G., Ewing, R.C. and D. Mohrig (2010), How do bedform patterns arise?
599 New views on the role of bedform interactions within a set of boundary conditions,
600 Earth Surf. Process. Landforms 35, 51–63, DOI: 10.1002/esp.1913

601 Krumbein, W. C. (1941) Measurement and geological significance of shape and
602 roundness of sedimentary particles. J. Sedimentary Research 11 (2), 64-72.

603 Lacey, R. W. J., and A. G. Roy (2008), The spatial characterization of turbulence
604 around large roughness elements in a gravel-bed river, Geomorphology, 102(3–4),
605 542–553, doi:10.1016/j.geomorph.2008.05.045.

606 Lague, D. (2010), Reduction of long-term bedrock incision efficiency by short-term
607 alluvial cover intermittency, J. Geophys. Res., 115, doi:10.1029/2008JF001210.

608 Lisle, T.E. (1995) Particle-size variations between bed-load and bed material in
609 natural gravel-bed channels, Water Res. Res. 31, 1107-18, doi:
610 10.1029/94WR02526

611 Nelson P. A., Venditte J. G., Dietrich W. E., Kirchner J. W., Ikeda H., Iseya F., and
612 L.S. Sklar (2009). Response of bed surface patchiness to reductions in sediment
613 supply. J. Geophys. Res. 114, F02005, doi: 10.1029/2008JF001144

614 Nelson, P. A., and G. Seminara (2012), A theoretical framework for the
615 morphodynamics of bedrock channels, Geophys. Res. Lett., 39, L06408,
616 doi:201210.1029/2011GL050806.

617 Papanicolaou, A. N., C. M. Kramer, A. G. Tsakiris, T. Stoesser, S. Bomminayuni,
618 and Z. Chen (2012), Effects of a fully submerged boulder within a boulder array on
619 the mean and turbulent flow fields: Implications to bedload transport, Acta Geophys.,
620 60(6), 1502–1546, doi:10.2478/s11600-012-0044-6.

621 Richardson K., Benson I. and P. A. Carling (2003). An instrument to record sediment
622 movement in bedrock channels. In: Erosion and Sediment transport measurement in
623 rivers: Technological and methodological advances (Proceedings of the Oslo
624 Workshop, June 2002). IAHS Publ. 283, 2003.

625 Seminara, G. (2010), Fluvial Sedimentary Patterns, *Annual Review of Fluid*
626 *Mechanics*, 42, 43-66.

627 Siddiqui, A and Robert, A. (2010), Thresholds of erosion and sediment movement in
628 bedrock channels, *Geomorphology*, 118, 301-13, doi:
629 10.1016/j.geomorph.2010.01.011

630 Sklar, L. S., and W. E. Dietrich (2004), A mechanistic model for river incision into
631 bedrock by saltating bed load, *Water Resources Research*, 40, W06301,
632 doi:10.1029/2003WR002496.

633 Strom, K., A. N. Papanicolaou, E. Evangelopoulos, and M. Odeh (2004), Microforms
634 in Gravel Bed Rivers: Formation, Disintegration, and Effects on Bedload Transport,
635 *Journal of Hydraulic Engineering*, 130(6), 554–567, doi:10.1061/(ASCE)0733-
636 9429(2004)130:6(554).

637 Strom, K., and A. Papanicolaou (2007), ADV Measurements around a Cluster
638 Microform in a Shallow Mountain Stream, *Journal of Hydraulic Engineering*, 133(12),
639 1379–1389, doi:10.1061/(ASCE)0733-9429(2007)133:12(1379).

640 Tan, L., and J. Curran (2012) Comparison of turbulent flows over clusters of varying
641 density, *Journal of Hydraulic Engineering* 138 (12), 1031-1044.

642 Turowski, J. M., N. Hovius, A. Wilson, and M.-J. Horng (2008), Hydraulic geometry,
643 river sediment and the definition of bedrock channels, *Geomorphology*, 99), 26–38,
644 doi:10.1016/j.geomorph.2007.10.001.

645 Turowski, J. M., D. Lague, and N. Hovius (2007), Cover effect in bedrock abrasion: A
646 new derivation and its implications for the modeling of bedrock channel morphology,
647 *J. Geophys. Res.*, 112(F4), doi:10.1029/2006JF000697.

648 Werner B.T. (2003), Modeling landforms as self-organized, hierarchical dynamical
649 systems. In *Prediction in Geomorphology*, Wilcock PR, Iverson RM (eds).
650 Geophysical Monograph 135, American Geophysical Union: Washington; 133–150

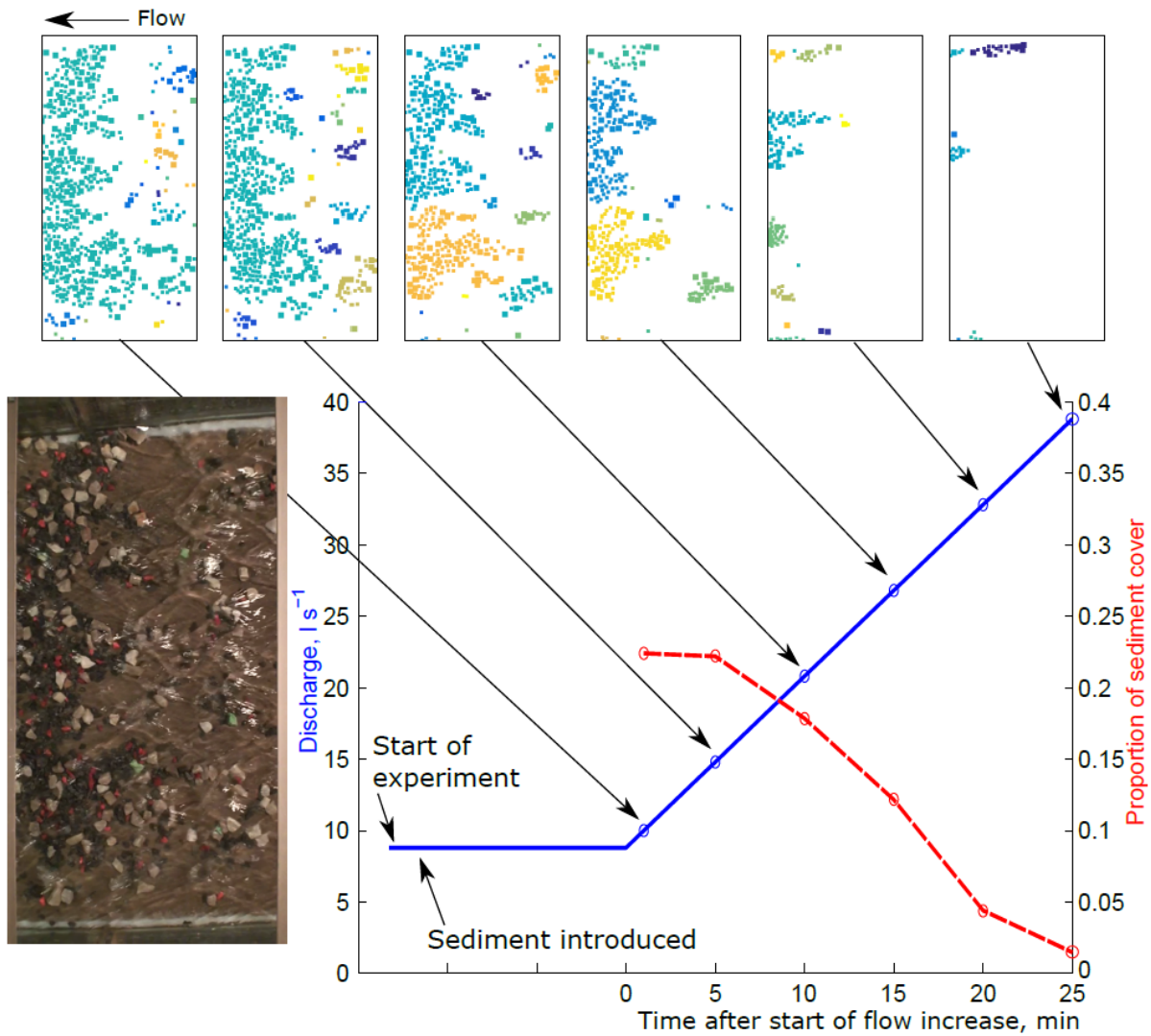
651 Werner, B. T., and T. M. Fink (1993), Beach cusps as self-organized patterns,
652 *Science*, 260(5110), 968–971.

653 Wohl, E.E. (2015), Particle dynamics: the continuum of alluvial to bedrock river
654 segments, *Geomorphology* 241, 192-208, doi:10.1016/j.geomorph.2015.04.014
655

Experimental property	Set		
	1	2	3
Sediment mixtures	Single grains C and F	100C	100C, 75C/25F, 50C/50F, 25C/75F, 10C/90F & 100F
Sediment size(mm)	Coarse = 15	Coarse = 15	Coarse = 15

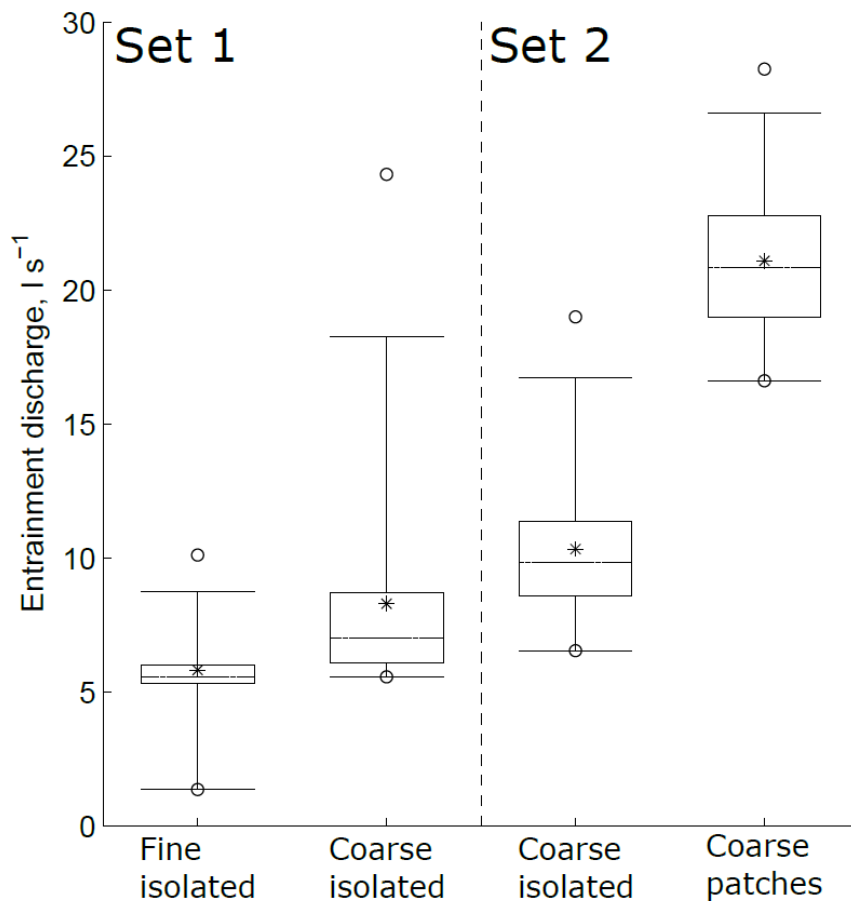
	Fine = 8.5		Fine = 8.5
Sediment mass supplied per run (kg)	single grain	20	6
Bed slope	0.0067	0.0050	0.0067
Flow rate during patch development (l s^{-1})	n/a	7.5 – 8.5	8.8
Flow depth (mm)	9 – 20 (F) 15 – 35 (C)	~30 (input) ~ 50 – 80 (final erosion)	~ 20 – 40 (input) ~ 50 – 80 (final erosion)
Time for sediment cover to develop (min)	n/a	~15	~15
Time for erosion (min)	n/a	~30	~30
Number of repeats	Coarse: 25 Fine: 25	21	100F: 5 100C & 10C/90F: 3 Others: 4

656 Table 1: Properties for the experimental runs.



657

658 Figure 1: Outline of the experimental procedure used in all experiment runs. In Set 1,
 659 individual grains were introduced, whereas in Sets 2 and 3 volumes of sediment
 660 were added. Insets show examples of digitised grains, taken from video stills of the
 661 measurement area. A patch is defined such that all grains in a patch are less than
 662 one grain diameter from a neighbouring grain. Different patches are shown with
 663 different colours, but colours are not consistent between time periods. Video stills
 664 and proportion of sediment cover data are from a 50C/50F run. The inset photo is of
 665 the bed at 1 minute into the increase in flow.



666

667 Figure 2: Distributions of discharges at which grains in Set 1 (n=25) and Set 2 (n=21)

668 experiments were entrained. Set 1 consisted of individual grains, whereas Set 2

669 comprised a mixture of isolated grains and sediment patches. For Set 2, the

670 discharge is that at which sediment started moving. Whiskers show 5th and 95th

671 percentiles, circles show minimum and maximum, and stars show mean. In Set 1 the

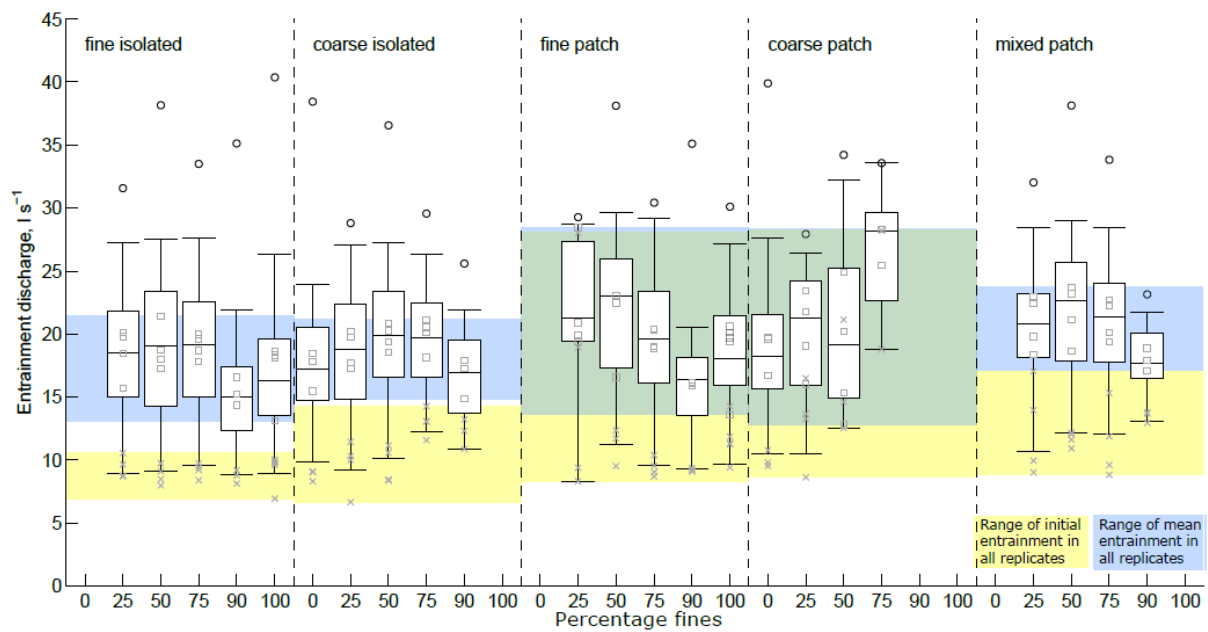
672 difference in entrainment discharge between fine and coarse grains is statistically

673 significant (t-test, 0.007), as is the difference between coarse isolated and coarse

674 patch grains in Set 2 (t-test, p < 0.0001). The difference between the entrainment

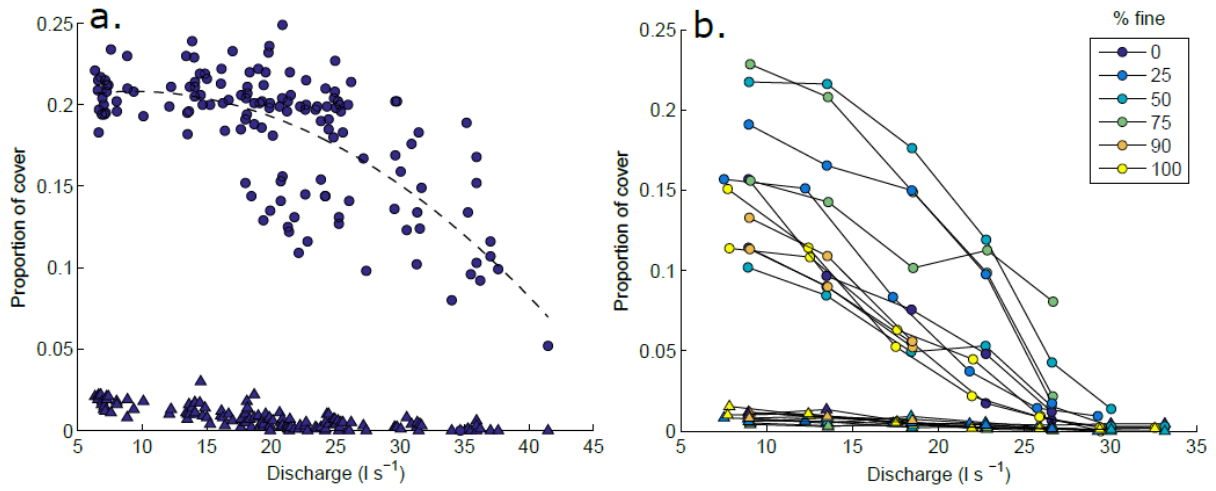
675 discharge for coarse isolated grains in Set 1 and Set 2 is not statistically significant

676 (t-test, p = 0.057).



677

678 Figure 3: Distributions of discharges at which grains were entrained in Set 3
 679 experiments. Data are grouped by sediment mixture, and grain size and location.
 680 The box plots show the combined data from all replicates with that sediment mixture.
 681 Whiskers show 5th and 95th percentiles, and black circles show maximum. Grey
 682 crosses and squares respectively show minimum and mean values from individual
 683 replicates; there is more variability for sediment in patches than for individual grains.
 684 The Kruskal-Wallis test indicates a significant difference ($p < 0.05$) between the
 685 minimum discharges for different grain sizes and positions in runs 100C/0F,
 686 10C/90F, 50C/50F and 25C/75F. The Kruskal-Wallis test also shows that, for each
 687 sediment mixture, there are significant differences between the full distributions of
 688 entrainment discharges for grains in different locations ($p \leq 0.02$).

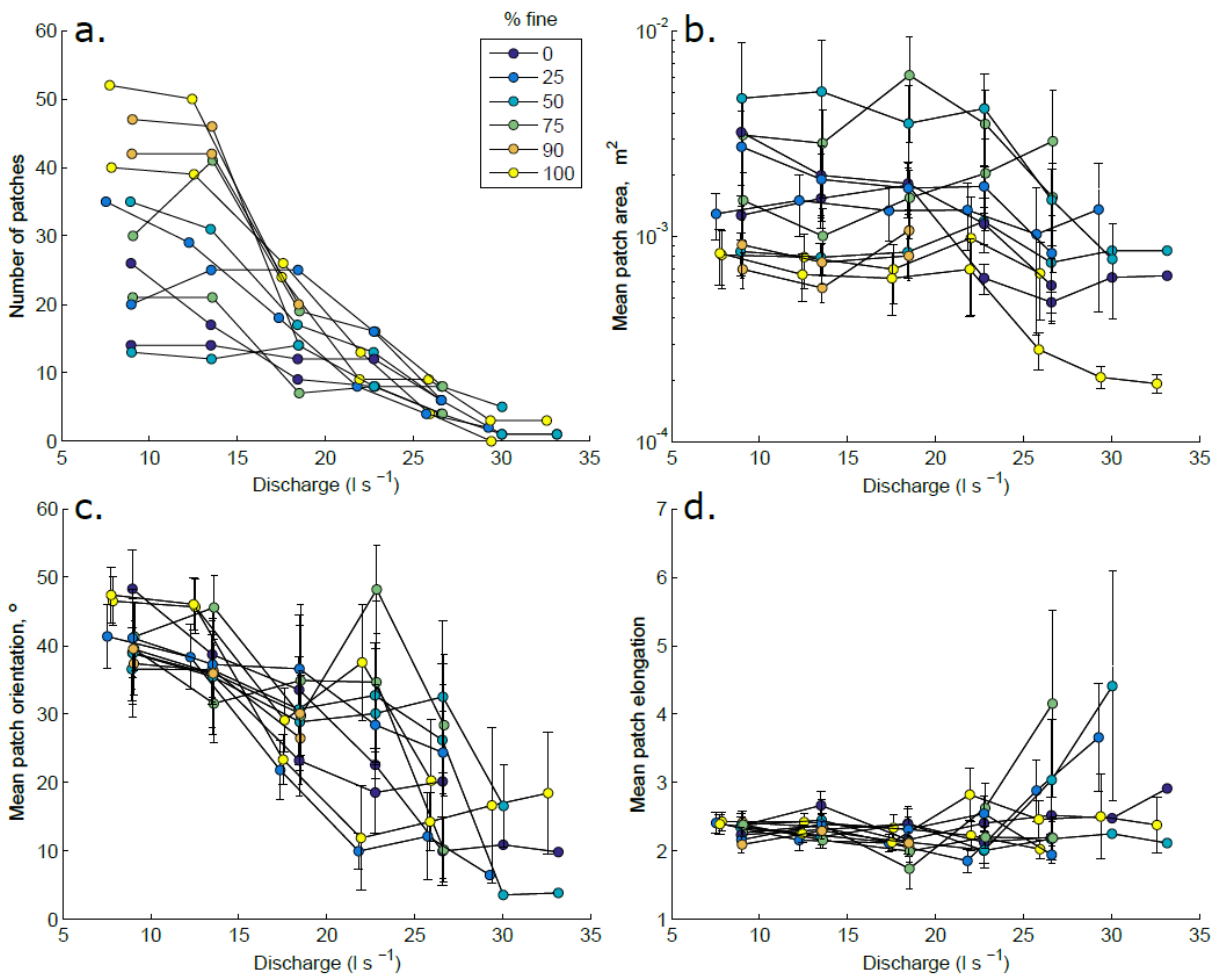


689

690 Figure 4: Decrease in sediment cover with increasing discharge for experiments in a)

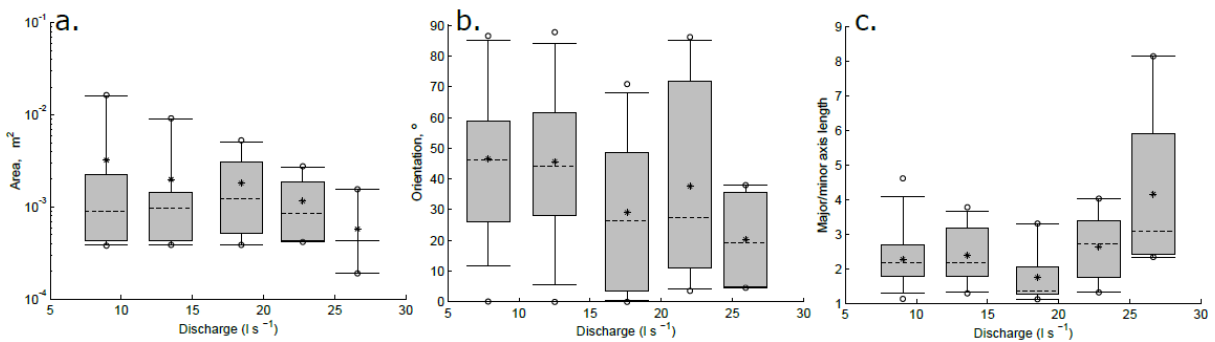
691 Set 2 and b) Set 3. In both, circles are cover from patches and triangles are cover

692 from isolated grains. Dashed line in a) shows a polynomial fit to the patch data.

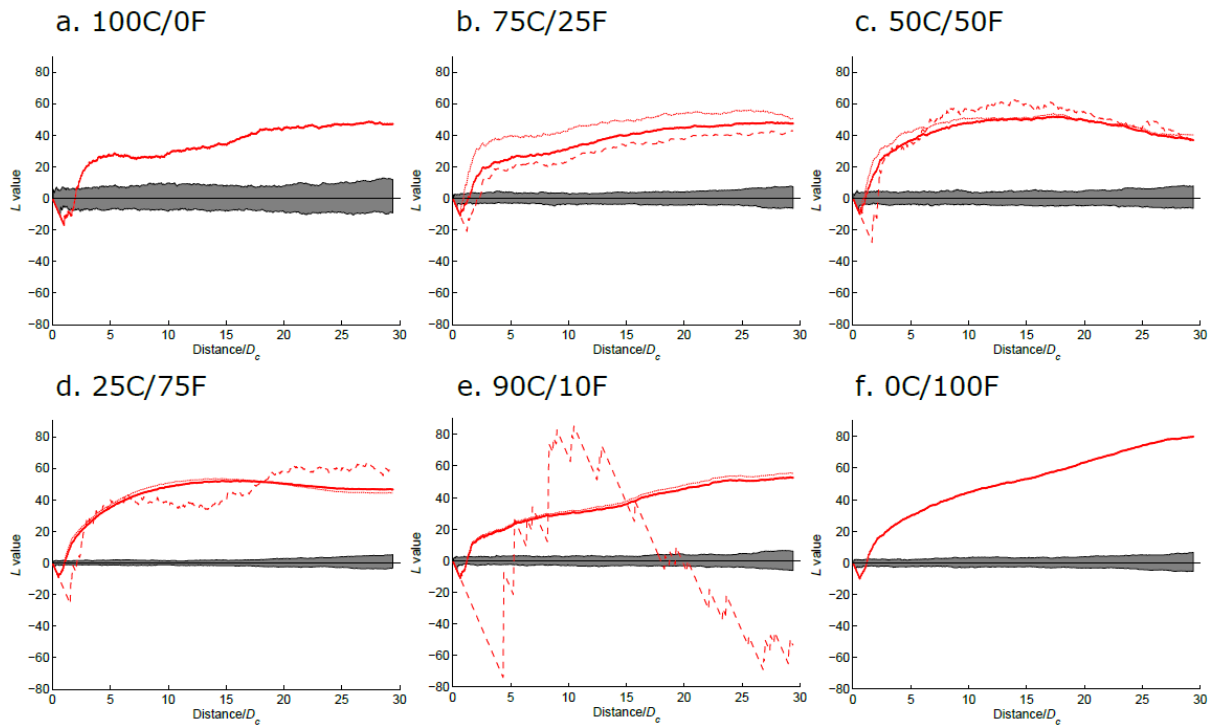


693

694 Figure 5: a) Number of patches, b) mean patch area, c) orientation and d) elongation
 695 as a function of changing discharge for selected Set 3 experiments. Orientation is
 696 measured relative to the downstream direction: 90° is perpendicular to flow and 0°
 697 parallel to flow. Area is the total bed area containing all the patch grains, not just the
 698 area of the grains themselves, and so includes areas of exposed bed within the
 699 patch outline. Elongation is the ratio of the lengths of patch major to minor axes.
 700 Error bars are one standard error of the mean.



701
 702 Figure 6: Examples of the changes in patch properties as a function of increasing
 703 discharge. In a. and b. there is a significant difference between the distributions
 704 (Kruskal-Wallis, $p < 0.05$). c. shows a representative example, but the differences
 705 are not significant.



706

707

708

709

710

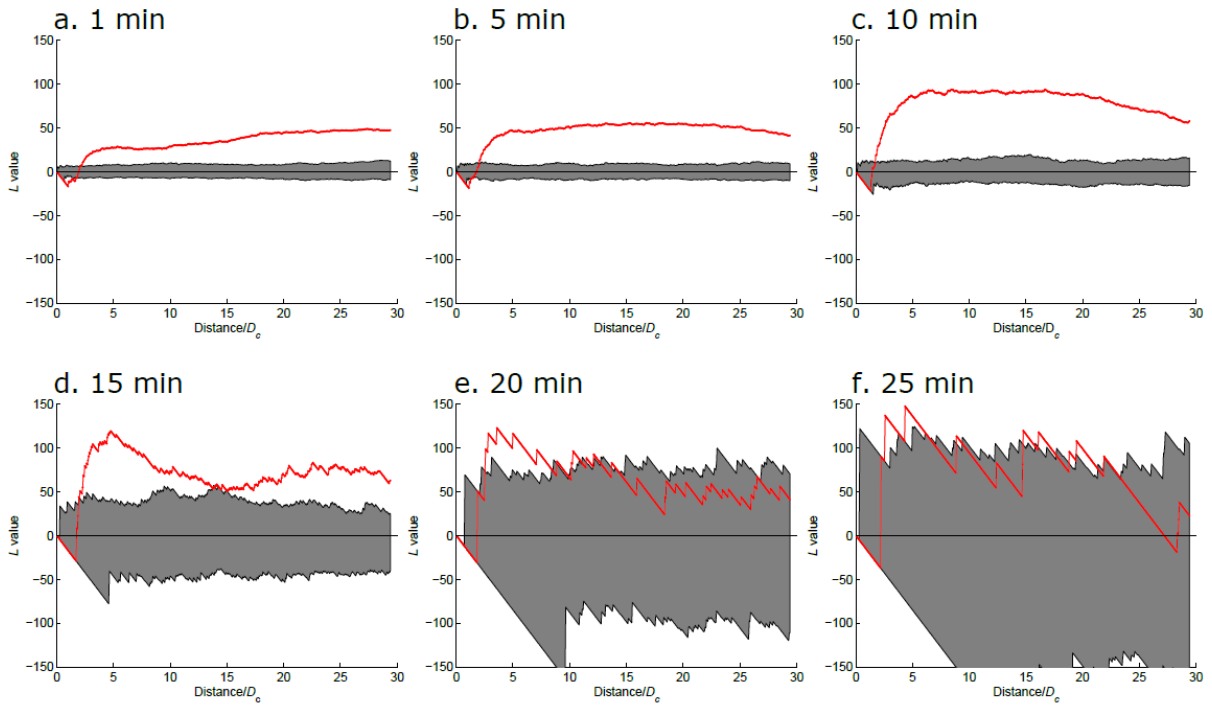
711

712

713

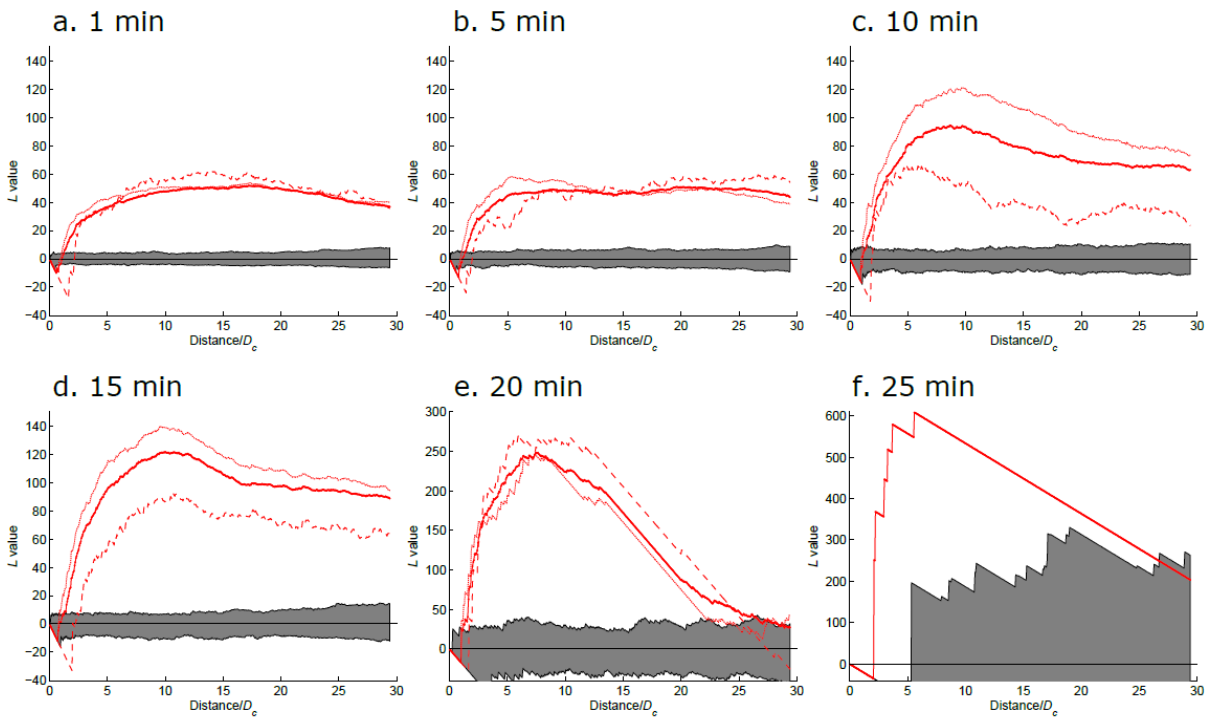
714

Figure 7: Values of Ripley's L at increasing spatial lags for the sediment grain distributions one minute into the flow increase. Values greater than zero indicate greater clustering than random, and values less than zero indicate greater dispersion than random. Solid line is for all grains. Fine line with short dashes is just fine grains, fine line with large dashes is just coarse grains. Grey areas are a 95% confidence interval, calculated from 100 repeat simulations with random spacing of n grains (where n is the number of digitised grains). Grain diameter (D_c) is the coarse grain diameter in all cases.



715

716 Figure 8: Values of Ripley's $L(r)$ at increasing spatial lags for the sediment grain
 717 distributions at increasing discharge in run 100C/0F. See caption of Figure 7 for
 718 further information.



719

720 Figure 9: Values of Ripley's $L(r)$ at increasing spatial lags for the sediment grain
721 distributions at increasing discharge in run 50C/50F. See caption of Figure 7 for
722 further information. Note different vertical axis scales in e. and f.

723